Synthesis of hydrometallurgical processes for valorization of secondary raw materials using ant colony optimization and key performance indicators

Vasilyev Fedor, Virolainen Sami, Sainio Tuomo

DOI: 10.1016/j.hydromet.2015.02.004

Synthesis of hydrometallurgical processes for valorization of secondary raw materials using ant colony optimization and key performance indicators

Fedor Vasilyev, Sami Virolainen, Tuomo Sainio*

Lappeenranta University of Technology, Laboratory of Separation Technology, Skinnarilankatu 34, FI-53850 Lappeenranta, Finland

*) *Corresponding author:* Phone: + 358 40 3578683. Email: tuomo.sainio@lut.fi

ABSTRACT

An algorithm-based method for synthesis of hydrometallurgical processes using limited amounts of experimental data is presented. The method enables simultaneous selection and sequencing of unit operations and optimization of operating parameters. An ant colony optimization (ACO) based algorithm is used to identify the most economic process alternative in an iterative manner. Key performance indicators are used for comparison of candidate processes: a purification performance index measures purity improvement and a separation cost indicator is used as an objective function in process optimization. Computational times were reduced significantly with the suggested method compared to an algorithm which evaluates all the possible process options. The practical applicability of the method to hydrometallurgy is demonstrated by investigating zinc recovery from argon oxygen decarburization dust with two alternative leaching methods and recovery of lanthanides from nickel metal hydride (NiMH) batteries. In the first zinc recovery process, 150 min normal batch leaching with 0.5 M H_2SO_4 is used, and in the other one 270 min batch leaching with H_2SO_4 is done by controlling the pH (>3.0). In both cases the leachate is extracted with D2EHPA at pH 4.27, and stripped with circulating solution from zinc electrolysis. For lanthanides recovery the algorithm suggested a process in which the raw material is leached with 1.3 M HCl, the leachate is extracted with D2EHPA at pH 2.2, organic phase is stripped with 2.0 M HCl and 99% pure Ln-oxalates are precipitated with oxalic acid at pH 0.6. Compared to previously suggested process for the same raw material, the algorithm suggests operating the leaching step such that higher selectivity is achieved by sacrificing some yield.

Keywords:

Process synthesis; Process development; Ant colony optimization; Dust treatment; Rare earth elements

Abbreviations

ACO	ant colony optimization
AOD	argon oxygen decarburization
CPU	central processing unit
EDR	energy dissipation rate
IRR	internal rate of return
KPI	key performance indicator
PPI	purification performance index
SCI	separation cost indicator

Notation

A	flow rate, m^3/s
c_i	concentration of contaminants, kg/m^3
E	concentration of extractant, m^3/m^3
K	cost, item of expenses, €/kg
k_L	specific cost of a leaching step, €/kg
$k_{pur,l}$	specific cost of a purification step, €/kg
L	probability
M	number of components in a chemical system
N	number of ants in a colony
n	number of process steps
P	number of discrete values of operating parameters
SL	solvent loss in solvent extraction
T	concentration of a target metal in the system, kg/m^3
t_b	batch time in leaching, s
U	number of unit operations
V_L	volume of leaching vessel, m^3
x	purity
Y	yield

Greek symbols

α	the degree of importance of the pheromones
ξ	parameter used to control the scale of the global updating of the pheromone
$\tau_{l,u,p}$	amount of pheromone in a cell
ρ	pheromone decay factor

Subscripts

0	initial
b	batch
chem	chemicals
el	electricity
extr	extractant
f	final
i	contaminant

L	leaching
l	process step
org	organic phase
p	value of operating parameter
raf	raffinate
sol	solvent
str	stripping
tot	total process SCI
u	unit operation

Superscripts

a	aqueous phase
k	ant
raf	raffinate

1. Introduction

Hydrometallurgical process development usually starts with analysis of the raw materials to be treated, i.e., chemical composition, mineralogy, state, particle size, volume etc. (Forsén and Aromaa, 2013). The process itself typically consists of three consecutive main steps: leaching, concentration and purification, and final product recovery. Several alternative unit operations are available for each process step. For instance solvent extraction, ion exchange, and/or selective precipitation can be employed for purification and concentration, and crystallization, chemical precipitation or electrowinning for product metal recovery. Moreover each unit operation can be run under a wide range of operating conditions (pH, pressure, phase ratio, solvent type, etc.). A key to successful and efficient hydrometallurgical purification is identification of the most suitable sequence of unit operations and the most effective combination of operating parameters to obtain the desired purification and yield with minimum (economical) effort.

Cisternas (1999) identified lack of works devoted to design of complete process due to complexity of the problem and great number of variables and restrictions to consider in his extensive review on synthesis of processes in extractive metallurgy and inorganic chemistry. To decrease the size of the problem process steps are usually designed individually (Cisternas, 1999), so that there are many methods and techniques available for design of each process step (Gálvez et al., 2004; Alonso et al., 2001; Trujillo et al., 2014). However, synthesis of complete processes is potentially more efficient since process step interactions are taken into account (Angira and Babu, 2006, Cisternas, 1999).

When a new hydrometallurgical process is being developed, comparison between process alternatives and process optimization is usually done based on the experience of scientists and engineers, as well as on extensive experimentation (Rintala et al., 2011). Over-expenditure on reagents, experiental biases, complicated data processing and the complexity of considering several process parameters simultaneously prolong the course of hydrometallurgical process development at its early stages and contribute to inefficiency.

Hydrometallurgical purification process development is usually based on scale-up of processes established on a laboratory or pilot scale. Conceptual design or process synthesis in the early stage is thus viewed as the most important stage of process development (Cziner et al., 2005). Major decisions affecting the lifecycle of the process are made during development of the first process flowsheet. Experience-based process synthesis can often result in overall suboptimal processes with inefficient utilization of energy and auxiliary

materials (Nfor et al., 2009). Therefore, systematic process development based on identification of justified optima is essential for efficient utilization of time and resources.

Nfor et al. (2009) identified four types of process synthesis strategies applicable to chemical industries: heuristics or knowledge-based strategies (Cziner et al., 2005), optimization-based strategies (Steimel et al., 2013; Grossmann and Daichendt, 1996), high-throughput experimentation strategies (Bhambure et al., 2011; Schuldt and Schembecker, 2013) and a combination of the afore-mentioned strategies (Ahamed et al., 2006). Each approach has strengths and weaknesses as discussed elsewhere (Nfor et al., 2009). Mathematical optimization based method can offer significant advantages to hydrometallurgical process development: clarification of interactions between unit operations, utilization of validated models for process optimization, user-independence after formulation of the search space, and the ability to identify the optimal process meeting the set criteria (Nfor et al., 2009). Application of mathematical optimization requires a superstructure of process alternatives and the availability of useful objective functions.

Numerical measures for assessment of process performance are required for efficient application of optimization based method. These measures have to reflect the main features of the alternative unit operations and form a reliable base for comparison. The main criteria for decisions on process synthesis in extractive metallurgy are technical feasibility and economic potential, along with environmental, safety and other aspects (Linninger, 2002; Chakraborty et al., 2004). It is desirable to base process synthesis decisions upon costs over the complete process. However, at the very beginning of process development, before process concepts are available, such information is not available and the profitability of a process or its internal rate of return (IRR) cannot be precisely estimated. The use of the key performance indicators (KPIs) introduced by Winkelnkemper and Schembecker (2010) offers a potentially effective approach to address this problem. The KPIs were developed for rating purification and cost-efficiency on the basis of single step purity improvement, yield and specific costs. The indicators do not require complete mass and energy balances and can be applied from the beginning of experimental investigation. Although the KPIs were first introduced for evaluation of pharmaceutical bio-separation processes, they are equally valid for hydrometallurgy.

Solution of an optimization problem requires a suitable and efficient algorithm that is capable of identifying the minimum value of the target function and the corresponding sequence of unit operations and their operating parameters. Mathematical programming algorithms and methods available for synthesis of chemical processes have been the subject of a number of reviews (Grossmann and Daichendt, 1996; Grossmann et al., 1999; Acevedo and

Pistikopoulos, 1998). Algorithms based on extensive searches for the optimal solution are computationally not preferred due to the high computational efforts required (Raeesi et al., 2008). However, the problem can be addressed in an efficient manner by using meta-heuristics to find approximate solutions (Raeesi et al., 2008; Biswas et al., 2009). The stochastic meta-heuristic ant colony optimization (ACO) algorithm has been found to be promising for efficient synthesis and optimization of processes (Raeesi et al., 2008; Chunfeng and Xin, 2002).

The objective of this research was development of an algorithm-based method for synthesis of hydrometallurgical processes using experimental data. Key theoretical aspects of *in silico* hydrometallurgical process development using ant colony optimization (ACO) and key performance indicators (KPIs) are discussed and the developed method and algorithm are presented. The efficiency of the algorithm is demonstrated, and utilization of the method is examined based on two case studies, namely recovery of Zn from argon oxygen decarburization (AOD) dust, and extraction of lanthanides from spent nickel metal hydride (NiMH) batteries.

2. Methods

The proposed method for design and optimization of hydrometallurgical purification processes consists of five steps:

- feed characterization and product specification,
- preselection of unit operations and the mass separation agents,
- collection of data (experiments or literature search for missing data),
- automated process synthesis,
- verification and validation of the constructed process.

In the first step, the specific characteristics of the purification process are set, e.g., the composition of the raw material, target purity, target concentration and other constraints. Based on these, a number of promising separation unit operations and corresponding mass separation agents are preselected. The latter are experimentally investigated by data collection experiments (construction of ad- and desorption isotherms, concentrations in leaching versus time or pH, step yields, changes of concentrations, etc.). The missing data can be also collected using literature search. The acquired data are used for simultaneous design and optimization of a purification process by means of a developed ACO-based algorithm and the synthesized process is then studied and developed further.

A hydrometallurgical process chain is built of individual unit operations: leaching, solvent extraction, stripping, chemical precipitation, etc. However, in general the unit operations are considered in the ACO-based algorithm as black boxes with inputs and outputs, and could just as well be continuous (e.g. SX) and even consist of multiple stages. An output from a unit operation is an input for the next one in the constructed process chain, i.e., the yield from one unit operation affects the feed composition of the next one. A model for each unit operation comprises mass balance equations.

2.1. Ant colony optimization

ACO is a probabilistic technique for solving computational problems (Blum, 2005). The algorithm is inspired by the foraging behavior of ants. Indirect communication between the ants by means of chemical pheromone trails is the core of this behavior. The pheromone trails enable the ants to find short paths between their nest and food sources. In the same way, ACO is usually used to find the shortest path from “nest” to “food” or from the first cell to the last one on the graph. Several possible routes through the different cells are first tried, but the shortest ones stand out. The ACO was used among others for optimization of chemical synthesis (Raeesi et al., 2008) and for design of multiproduct batch chemical process (Chunfeng and Xin, 2002). The same principles can be implemented for defining an optimum hydrometallurgical process sequence. A cost function, which represents the dependence of the specific costs of the final product on the composition of the raw materials and the unit operation parameters, is used as an objective function for optimization.

2.1.1. Algorithm development

The hypothetical ants travel through a multi-layered structure (Fig. 1). The path of the ant corresponds to a solution of the design problem as it determines the sequence of unit operations and their operating parameter for every process step. The composition of aqueous, organic or solid phases is calculated based on the chosen unit operation and the values of its operating parameters. The search domain consists of n layers which represent the prespecified number of process steps. On each layer every ant has to choose a cell *pu* that represents a unit operation with its operating parameters, for instance solvent extraction with equilibrium pH 3.0 or leaching with 2.0 M HCl. For each hydrometallurgical purification process, U candidate unit operations with P operating parameters are nominated. The number of discrete operating parameters P depends on the size of the available data set. If needed, experimental data can be interpolated to get a sufficient number of discrete values. Consequently, the search domain consists of $n \cdot U \cdot P$ cells, which means $(U \cdot P)^n$ possible processes.

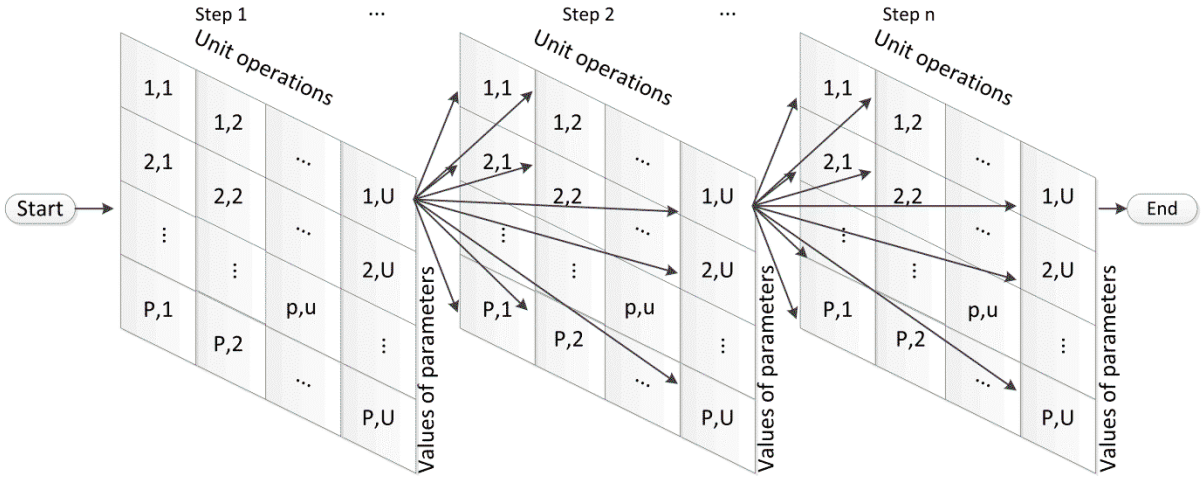

Figure. 1. Graphical representation of the ACO search in the form of a multi-layered structure, with *n* process steps, *U* unit operations and *P* discrete values of operating parameters for each unit operation.

The main features of the devised ACO-based algorithm are given as a flow chart in Fig. 2. Identification of the best solution is an iterative process. In each iteration, *N* hypothetical ants travel from the start point to the end point of the graph. Each iteration starts from launching the first ant and ends by updating the pheromone matrix in compliance with evaluation of solutions constructed by the hypothetical ant colony in the iteration. On the initialization step a three-dimensional matrix corresponding to ACO search network (Fig. 1) is created. It contains the collected experimental data and all the processes that can be constructed are present there. Also the matrix containing pheromone values is created of the same size. Every hypothetical ant travels through the graph selecting one cell on each layer consequently creating a process route. All the process routes created by every ant from the colony constitute the superstructure of the solutions. All the process routes from the superstructure are being evaluated and the best one is identified. The iterative search stops when all ants construct the same process route.

2.1.2. Layer transition and pheromone updating rules

The layer transition rule determines the probability of choosing a cell on each process step. The probability relies on the pheromone value, $\tau_{l,u,p}$, assigned for each cell of the search domain. The probability of selecting of a certain cell on a certain layer is defined according to amount of pheromone it contains comparing to other cells on the same layer (roulette wheel selection mechanism) (Rao, 2013):

$$L_{\mathrm{l,u,p}} = \frac{\tau_{\mathrm{l,u,p}}}{\sum_{u=1}^{U}\sum_{p=1}^{P}\tau_{\mathrm{l,u,p}}} \tag{1}$$

As the raw materials are solids in the cases considered in this paper, prior to the first iteration the pheromone is uniformly distributed over the search domain in such a way that only leaching can be chosen as a unit operation of the first layer. In addition, heuristics and a phase selection rule are applied in the ACO-based algorithm to govern the selection of successive unit operation. The former one renders the logic of hydrometallurgical process synthesis and determines, for example, that only solvent extraction or precipitation can follow the leaching step and not stripping. The later one postulates that the phase with yield of target element more than 50% is subjected for further treatment. The heuristics and the rule are realized by respective pheromone redistribution for each hypothetical ant before it makes a decision on the next layer.

After each iteration, the pheromone value of each cell is updated according to the pheromone updating rule Eq. (2) (Rao, 2013). One iteration is a complete cycle involving the ant's movement, pheromone evaporation and pheromone deposition. The goal of the pheromone update is to increase the pheromone value associated with good or promising paths.

$$\tau_{\mathrm{l,u,p}} = (1-\rho)\cdot\tau_{\mathrm{l,u,p}} + \sum_{\mathrm{k}=1}^{\mathrm{N}}\Delta\tau_{\mathrm{l,u,p}}^{(\mathrm{k})} \tag{2}$$

where $\Delta\tau_{l,u,p}^{(k)}$ is the amount of pheromone deposited on cell *pu* by the best ant *k*, *i.e.*, by the ant with the minimum value of the objective function, and $\rho \in [0, 1)$ is the pheromone decay factor. The decrease in pheromone intensity favors the exploration of different paths during the search process, which assists elimination of poor choices made previously. Furthermore, it helps in bounding the maximum value attained by the pheromone trails.

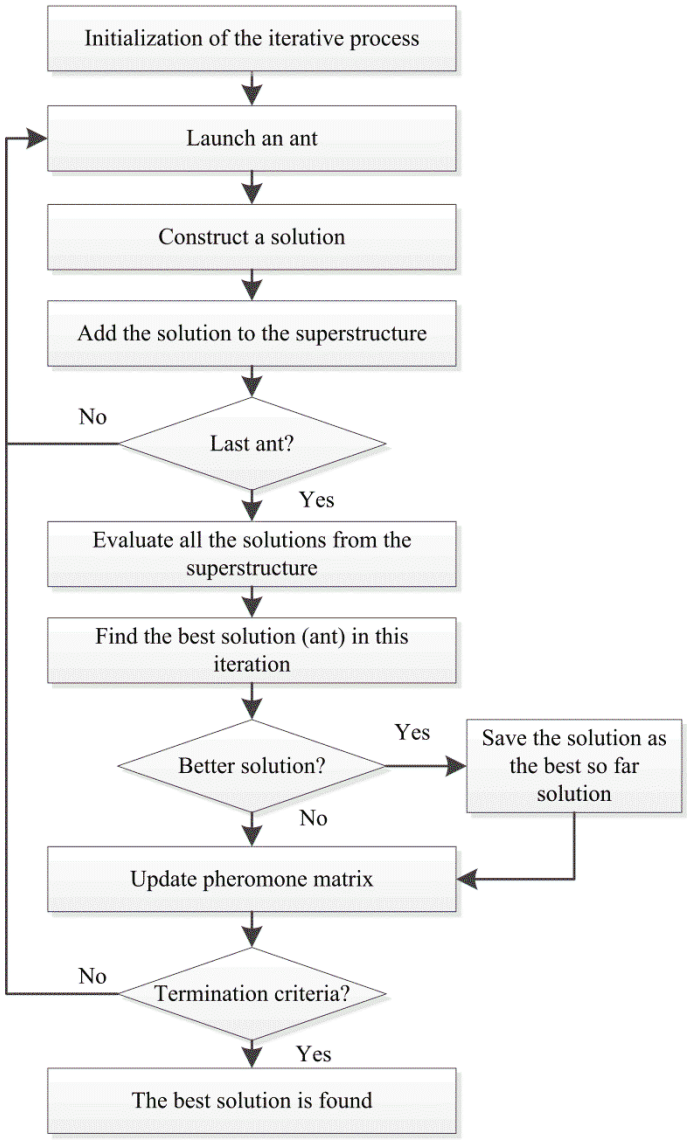

Figure 2. Flow chart for an ant colony optimization (ACO) based algorithm.

At the end of an iteration, when each ant has chosen a cell on each layer, i.e., after construction of the solutions superstructure, the constructed processes have to be evaluated and compared to identify the best one. SCI function, which represents dependence of specific costs of final product on composition of raw materials and unit operation parameters, is used as an objective function for optimization. The pheromone deposited on cell *lup* by the best ant *k* is taken as (Rao, 2013)

$$\Delta\tau_{l,u,p}^{(k)} = \begin{cases} \dfrac{\xi \cdot SCI_{best}}{SCI_{worst}} & \text{if } l,u,p \in \text{global best path} \\ 0 & \text{otherwise} \end{cases} \quad (3)$$

where SCI_{worst} is the worst value and SCI_{best} is the best value of the objective function among the paths taken by the *N* ants, and ξ is a parameter used to control the scale of the global

updating of the pheromone. The larger the value of ξ, the more pheromone is deposited on the global best path, and the better the exploitation ability.

The pheromone decay factor ρ, the global updating scale parameter ξ and the population of the ant colony N are the principal parameters of the ACO algorithm. Values of these parameters may slightly change, depending on the problem size and complexity. The values $\rho = 0.1$ and $N = 2 \cdot U \cdot P$ were used, as Raeesi et al. (2008) showed that for a nonlinear combinatorial problem ACO algorithm finds the optimal solution with minimal computational effort with these values. The global updating scale parameter ξ was varied for each particular problem depending on scale of difference between SCI_{best} and SCI_{worst}. An empirically adjusted typical value was 1.5.

2.2. Key performance indicators (KPIs)

In order to evaluate the suitability of different process alternatives in the early stages of process development, selectivity and estimated relative costs or KPIs introduced by Winkelnkemper and Schembecker (2010) are applied. KPIs are suitable for initial stages of purification process design, where not enough data for rigorous optimization is available.

2.2.1. Purification rating

Purity, defined as the fraction of the target product in a mixture with contaminants, is an essential concept in description of performance and can be described by Eq. (4) (Winkelnkemper and Schembecker, 2010), where T is the concentration of a target metal in the system, c_{i} is the concentration of contaminant i, and M is number of metals in the system:

$$x = \frac{T}{T + \sum_{i=1}^{M-1} c_{\text{i}}} = \frac{1}{1 + \sum_{i=1}^{M-1} \frac{c_{\text{i}}}{T}}. \tag{4}$$

For assessment of the purification of one step as a percentage of the purification of the total process to be designed, the purity of the initial mixture x_0 and the target purity x_{f} must be considered as given boundaries of the purification process. The purification performance index (PPI_{j}) is defined as (Winkelnkemper and Schembecker, 2010):

$$PPI_{\text{l}} = \frac{\tanh^{-1}(2x_{\text{l}} - 1) - \tanh^{-1}(2x_{\text{l}-1} - 1)}{\tanh^{-1}(2x_{\text{f}} - 1) - \tanh^{-1}(2x_0 - 1)} \tag{5}$$

Due to high nonlinearity of arctangent function, *PPI* is a balanced measure of purity over the whole purity range of a purification process. It evenly rates purification process steps, when high purity improvement requires moderate effort, and conversion and recovery steps, when small purity improvement requires great effort. Thus *PPI* can be used to connect the purification performance with the projected effort. As the purity x is defined by the concentrations of all contaminants i (c_i) and the target substance (T) Eq. (4). PPI_l can be rearranged and expressed with the concentrations (Winkelnkemper and Schembecker, 2010):

$$PPI_l = \frac{\log\left(\sum_{i=1}^{M-1}\frac{c_{i,l}}{T_l}\right) - \log\left(\sum_{i=1}^{M-1}\frac{c_{i,l\text{-}1}}{T_{l\text{-}1}}\right)}{\log\left(\sum_{i=1}^{M-1}\frac{c_{i,f}}{T_f}\right) - \log\left(\sum_{i=1}^{M-1}\frac{c_{i,0}}{T_0}\right)} \tag{6}$$

Eq. (6) shows that *PPI* reflects changes in contaminant-to-target ratios.

2.2.2. Cost-estimation

As soon as a complete process concept is established, the influence of single purification steps on total process costs is readily quantifiable using a separation cost indicator (*SCI*). The separation cost indicator depends only on the normalized purification rating, yield (Y_l), and the specific costs (Winkelnkemper and Schembecker, 2010). In the present case, the specific costs are leaching cost, k_L, and the specific cost of purification steps, $k_{pur,j}$:

$$SCI_l = Y_l^{-\frac{1}{PPI_l}} \cdot \left(k_L + k_{pur,l} \cdot \frac{1 - Y_l^{\frac{1}{PPI_l}}}{1 - Y_l} \right) \tag{7}$$

Both *PPI* and *Y* are used as decimal fractions in Eq. (7) and the *SCI* function is determined for $Y \in [0,1)$ and $PPI \in [0,1)$. A major challenge is quantification of specific costs for the leaching and purification steps, since comparison of the process alternatives using SCI is only as reliable as the degree of precision of the estimation of these specific costs.

The optimization task of the purification process synthesis is minimization of total specific production costs for the process. Therefore, the sum of specific costs of the process steps is taken as the target function. The specific costs of the whole process are equal to the sum of step-specific costs of all purification steps within the process:

$$SCI_{tot} = \sum_{l=1}^{n} SCI_l \tag{8}$$

2.2.3. Determination of SCI for leaching and purification

For comparison purposes, the costs of alternative leaching processes, K_L, can be calculated using operational costs (Sreekrishnan and Tyagi, 1996):

$$K_L = \sum K_{equipment} + \sum K_{chemicals} + \sum K_{utilities} + \sum K_{labor} \quad (9)$$

Only the chemical costs and the costs of electricity required for mixing are here taken into account in estimation of specific costs of leaching step. Chemical costs are calculated based on the quantity of each chemical required for the process and its unit price. The quantity of acid needed is calculated from the process chemistry, the composition of the solids and its consumption in the process. The costs of mixing accounts electricity needed for slurry mixing. Both chemical and electricity costs are calculated per unit mass of target metal in the leachate.

$$k_L = k_{mixing} + k_{chem} \quad (10)$$

For simplification and generalization, operating costs of solvent extraction are here assumed to result from the introduction of the organic phase to the process stream, stripping by aqueous solution and power consumed in mixing and pumping of the phases. The function for calculation of the operating costs resulting from losses of the target compound and solvent, for both solvent extraction and stripping stages, is (Robinson and Paynter, 1971):

$$K_{pur,l} = A \cdot K_t \cdot T_l^{raf} + SL \cdot A \cdot \left(E \cdot K_{extr} + (1-E) \cdot K_{sol}\right) \quad (11)$$

where A is the feed rate of the aqueous phase, m^3/s; K_t is the price of target element, €/kg; T_l^{raf} is the concentration of the target element in the raffinate, kg/m^3; SL is the solvent loss per unit volume, m^3/m^3; E is the volume concentration of extractant, m^3/m^3; K_{extr} is the cost of extractant, €/m^3 and K_{sol} is the cost of diluents, €/m^3.

Pumping and mixing costs can be estimated from their ratio with reagent costs, as the operating costs of solvent extraction are stated as consisting of 89.9% reagents and 10.1% electricity (US Bureau of Mines, 2009). Therefore, dividing the operating costs by the final concentration of the target metal T_l the specific costs for the solvent extraction and stripping steps are:

$$k_{pur,j} = \frac{A_{raf} \cdot K_t \cdot T_l^{raf} + 1.11 \cdot SL \cdot A_{org} \cdot \left(E \cdot K_{extr} + (1-E) \cdot K_{sol}\right)}{T_l \cdot A_t} \quad (12)$$

where A_{raf} is the raffinate flow rate, m^3/s; A_{org} is the flow rate of organic phase, m^3/s and A_t is the flow rate of the phase containing major amount of the target metal, m^3/s.

2.3. Efficiency of the method

The ACO-based algorithm was implemented in Matlab. In order to demonstrate the efficiency of the method, calculation times were compared with an enumeration algorithm also implemented in Matlab. The latter constructs all possible combinations of process alternatives and operating parameters and finds the one with the lowest specific production costs for the target component using the SCI function. Arbitrary pyrity and yield data were used as inputs, and the number of process steps and operating conditions were varied to vary the total number of process alternatives.

As seen in Fig. 3, the ACO-based algorithm is significantly faster when the number of process alternatives is large. Typically, the solution is obtained with a few seconds, even when enumeration takes tens of minutes. For very small problems, the difference is not significant and enumeration can be faster.

The efficiency of the ACO-based algorithm in process synthesis originates from the fact that it identifies the best combination of process steps without evaluation of all possible process combinations. Instead, it performs selection of the best process options in an iterative manner, discarding the worst unit operations or operating parameters at the very beginning. Hence, it is possible to evaluate many processes and select the best one in a reasonably short time. The difference in calculation times would be even more critical if the computational effort required to evaluate the PPI and SCI on each layer was considerable. This is the case if dynamic simulations are involved or iterative solutions of sets of algebraic equations are required.

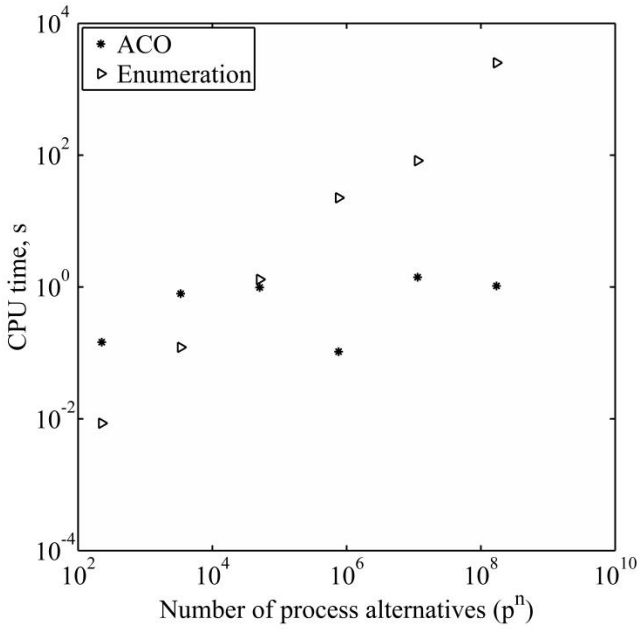

Fig. 3. Efficiency of the ACO-based algorithm compared to enumeration algorithm.

3. Results and discussion

In order to evaluate the proposed method and algorithm from hydrometallurgical point of view, two case studies are presented. The first case is synthesis of hydrometallurgical processes for Zn recovery from argon oxygen decarburization (AOD) dust. The second case focuses on hydrometallurgical recovery of lanthanides from spent NiMH batteries. Single stage batch unit operations are exclusively considered in the example case studies. The enumeration algorithm was employed to ascertain that the ACO-based algorithm has identified the optimal process, which was the case in both examples.

The original intention of the SCI was to rate single process steps in terms of the costs of the purification scaled up to 100% (Winkelnkemper and Schembecker, 2010). SCI is a step-specific economic rating in the context of a complete process that is unknown except for the boundary purities. In the current study, however, the SCI-function (Eq. 8), as the summation of step specific SCIs, is used as an objective function for the algorithm-based process synthesis, that is valid for the purpose of the initial process flowsheet synthesis. The intention is to estimate the total process costs on the basis of the costs of the separate process steps.

3.1. Zinc recovery from AOD dust

Argon oxygen decarburization (AOD) dust is generated in stainless steel production processes, and contains valuable heavy metals. Its composition is presented in Table 1. Based on previous work by Virolainen et al. (2013), Zn was chosen as the target component for recovery.

The most common way to produce metallic Zn in hydrometallurgy is by electrolysis of $ZnSO_4$ solutions (Habashi, 1997). The chemical composition of the electrolyte in the process has a significant influence on process performance and economics. The electrolyte is to contain 50-90 g/L of Zn and 120-200 g/L of H_2SO_4 (Tsakiridis et al., 2010), and typical impurity content of industrial electrolytes is: Fe 20-50 mg/L, Ni 0.1-0.5 mg/L, Mn <10 g/L, Na <10 g/L, Mg <10 g/L and other metals <20 mg/L (Marchenko, 2009). Using these limitations, the target purity of Zn can be calculated, according to Eq. (1), as 99.6%.

The process was constructed utilizing H_2SO_4 as the lixiviation agent. H_2SO_4 in low and moderate concentrations shows high yield and selectivity for Zn over Fe (Shawabkeh, 2010), and in high H_2SO_4 concentrations yields are even higher but some of the undesired Fe is also leached. Thus two routes were examined separately; a route in which the dust was leached directly in batch reactor with 0.5 M H_2SO_4, and a route in which the dust was leached by

488 controlling the pH with H_2SO_4 to be close to, but not below 3.0. Three extractants were
489 selected for purification of the AOD leachates: 25% v/v Di-(2-ethylhexyl)phosphoric acid
490 (D2EHPA) in kerosene, 10% v/v carboxylic acid Versatic 10 in *n*-heptane and 20% v/v
491 hydroxyoxime LIX 984 in xylene (Extraction data only for Zn, Ni, Fe and Pb were found in
492 the Rodríguez de San Miguel et al. (1997). Extraction of other metals from the leach solution
493 by extractant LIX 984 was assumed to be negligible.). Phase ratio was 1:1 for all the
494 extractants. Stripping of the loaded organic phase was done by spent electrolyte. Its metals
495 content is presented in Table 1 (Pereira et al., 1997).

496 Table 1. Composition of the raw material (AOD) and aqueous solutions in the recovery
497 process of Zn from AOD dust. The raw material contains 31.5% of other elements (mainly
498 oxygen) not listed here. The concentration of H_2SO_4 in Zn stripping solution is 181.3 g/L.

	Ca	Fe	K	Mg	Cr	Mn	Mo	Ni	Pb	Zn
Composition of raw material (Virolainen et al., 2013), %	4.78	38.3	0.93	1.25	9.74	2.76	0.03	0.72	0.10	9.93
Composition of Zn stripping solution (Pereira et al., 2007), mg/L	0.34	1.03	–	18.4	–	3.20	–	0.54	0.87	73600
Composition of the final purified solution in the process with direct leaching, mg/L	470	1560	72	403	20	804	0	1.3	0.9	86630
Composition of the final purified solution in the process with pH controlled leaching, mg/L	400	1	49	329	11	230	0	0.7	0.9	83940

499

500 Experimental data on leaching of AOD dust and solvent extraction were taken from literature
501 (Virolainen et al., 2013; Rodríguez de San Miguel et al., 1997; Preston, 1985) and are
502 presented in Appendix A. The available leaching data represent two modes of leaching: direct
503 leaching with H_2SO_4 (Fig. A1), and leaching with controlled pH of leachate above 3.0 to
504 prevent dissolution of Fe (Fig. A2). The data are expressed as concentrations of metals and
505 pH, depending on leaching time in a batch process. Therefore, the task is to find the optimal
506 time to dissolve Zn in the most economical way. For solvent extraction and stripping steps,
507 the data represent dependence of metals extraction on pH of aqueous phase, and the task is to
508 identify the most economical pH using yield and purity improvement as target quantities. For
509 calculation of stripping step, the same equilibrium data sets were used as for extraction step.
510

The developed ACO-based algorithm was used for simultaneous process design and optimization, i.e., for selection of the most economical sequence of unit operations and its operating parameters. A separation cost indicator (SCI) was used for evaluation of the process performance. Specific costs for the leaching (k_L) and purification ($k_{pur.j}$) steps are required for calculation of SCI. The values can be calculated according to Eq. (10) and Eq. (12).

Consumption of H_2SO_4 in the leaching can be estimated based on dissolution chemistry. The Zn dissolution reactions are the following (Havlik et al., 2005):

$$ZnO + H_2SO_{4(aq)} \rightarrow Zn^{2+} + SO_4^{2-} + H_2O \quad (13)$$

$$ZnFe_2O_4 + 4H_2SO_{4(aq)} \rightarrow Zn^{2+} + SO_4^{2-} + Fe_2(SO_4)_3 + 4H_2O \quad (14)$$

$$ZnFe_2O_4 + H_2SO_{4(aq)} \rightarrow Zn^{2+} + SO_4^{2-} + Fe_2O_3 + H_2O \quad (15)$$

$$CaO + H_2SO_{4(aq)} \rightarrow CaSO_4 + H_2O \quad (16)$$

Reaction (16) is assumed to go to completion. The leaching of Zn from its minerals is slower than formation of $CaSO_4$, so the consumption of H_2SO_4 depends on desired concentration of Zn in the leachate. In absence of other knowledge, it is assumed that zincite and franklinite are present in ratio of 1:2 in the AOD dust and thus six moles of H_2SO_4 are required for dissolution of three moles of Zn. Therefore, the concentration of H_2SO_4 (in units of g/L) needed is three times the desired final concentration of Zn in the leachate ($M_{H_2SO_4}/M_{Zn} = 1.5$). A considerable amount of H_2SO_4 is consumed also in reaction (16) as the dust contains 7% CaO. Consequently, the total amount of H_2SO_4 required is:

$$m_{H_2SO_4} = \frac{0.07 \cdot m_{AOD} \cdot M_{H_2SO_4}}{M_{CaO}} + 3 \cdot c_{Zn^{2+}} \cdot V_L \quad (17)$$

The specific cost of chemicals is then calculated as:

$$k_{chem} = \frac{K_{H_2SO_4}}{V_L \cdot c_{Zn^{2+}}} \left(\frac{0.07 \cdot m_{AOD} \cdot M_{H_2SO_4}}{M_{CaO}} + 3 \cdot c_{Zn^{2+}} \cdot V_L \right) \quad (18)$$

A value of 0.145 €/kg was used for the price of leaching acid, $K_{H_2SO_4}$, the volume of leaching vessel, V_L was 5 L, and the mass of the AOD dust was 0.8 kg. The concentration of Zn in the leachate, $c_{Zn^{2+}}$, is a time dependent variable and changes as leaching progresses.

We assume complete particle suspension in a severe agitation operation with energy dissipation rate (power input/unit mass) *EDR* = 1 W/kg slurry (Harnby et al., 1997). The specific costs of mixing (electricity) in leaching are:

$$k_{\text{mixing}} = \frac{EDR \cdot \rho_{\text{slurry}} \cdot K_{\text{el}} \cdot t_{\text{b}}}{60 \cdot c_{\text{Zn}^{2+}}} \quad (19)$$

where ρ_{slurry} is slurry density, kg/m^3; K_{el} is price of electricity, €/kWh; t_{b} is batch time in minutes and $c_{\text{Zn}^{2+}}$ is concentration of target metal in the slurry, kg/m^3.

Eq. (12) is used for calculation of the specific costs of the purification steps for both solvent extraction and stripping. In the case of Zn solvent extraction from leachate of AOD the equation takes the form:

$$k_{\text{SX,j}} = \frac{K_{\text{Zn}} \cdot c^{\text{raf}}_{\text{Zn}^{2+}} + 1.11 \cdot SL \cdot R_{\text{SX}} \cdot \left(E \cdot K_{\text{extr}} + \left(1 - E\right) \cdot K_{\text{sol}} \right)}{R_{\text{SX}} \cdot c^{\text{O}}_{\text{Zn}^{2+}}} \quad (20)$$

where R_{SX} is the organic to aqueous phase ratio in solvent extraction; $c^{\text{raf}}_{\text{Zn}^{2+}}$ is concentration of Zn in raffinate, kg/m^3 and $c^{\text{O}}_{\text{Zn}^{2+}}$ is concentration of Zn in organic phase, kg/m^3.

In the stripping stage, the costs for neutralization of stripping electrolyte with NaOH to the certain pH are taken into account, and thus Eq. (10) for the stripping of loaded organic phase takes the form:

$$k_{\text{Str,l}} = R_{Str} \cdot \frac{K_{\text{Zn}} \cdot c^{\text{raf}}_{\text{Zn}^{2+}} + 1.11 \cdot SL \cdot \left(E \cdot K_{\text{extr}} + \left(1 - E\right) \cdot K_{\text{sol}} \right)}{c^{\text{a}}_{\text{Zn}^{2+}}} + \frac{m_{NaOH} \cdot K_{NaOH}}{c^{\text{a}}_{\text{Zn}^{2+}}}, \quad (21)$$

where R_{Str} is the organic to aqueous phase ratio in stripping; $c^{\text{a}}_{\text{Zn}^{2+}}$ is concentration of Zn in the aqueous phase after stripping, kg/m^3; m_{NaOH} is mass of NaOH needed for neutralization of the electrolyte, kg, and K_{NaOH} is price of NaOH, €/kg.

The price of Zn is assumed to be 1.39 €/kg (LME spot price March 2014), the prices of D2EHPA and kerosene are assumed to be 2.32 €/L and 0.74 €/L (U.S. Energy Information Administration, 2014), the prices of Versatic 10 and xylene are assumed to be 1.59 €/L and 5.03 €/L, and prices of LIX 984 and *n*-heptane are assumed to be 7.89 €/L and 4.12 €/L. The solvent loss per unit volume is set to be 100 ppm (Cytec, 2006). The price of NaOH is assumed to be 0.34 €/kg. The price of electricity is taken as 0.087 €/kWh (Statistics Finland,

2014). Eqs. (18-21) are implemented in the algorithm for calculation of the SCI function according to Eq. (7).

The hydrometallurgical processes for the recovery of Zn from AOD dust constructed by the ACO-based algorithm is presented in Table 2. The design space (see graph in Fig. 1) consisted of 3 process steps, 8 unit operations and 30 levels of operating parameters for each step (linear interpolation of data was used). The number of alternative processes and operating parameter combinations is approximately $1.4 \cdot 10^7$ but, with ACO-based method, the CPU time was only 13 s. The short computational time to solve the current process synthesis problem can be explained by simplicity of the model, as only algebraic calculus are used, and by efficiency of the ACO in solving combinatorial optimization problems (Raeesi et al., 2008; Chunfeng and Xin, 2002).

Table 2. Constructed processes for recovery of Zn from AOD dust using ACO-based algorithm.

Leaching method: Direct						
Unit operation	Time, min	pH	O/A	Yield, %	PPI, %	SCI, €/kg
Leaching	150	3.0	–	68.7	36.1	2.02
SX	–	4.27	1	99.93	9.3	0.87
Stripping	–	<0	1	99.9	23.1	0.73
Total process				68.6	68.5	3.61
Leaching method: Controlled pH						
Unit operation	Time, min	pH	O/A	Yield, %	PPI, %	SCI, €/kg
Leaching	270	3.2	–	55.2	41.7	3.33
SX	–	4.27	1	99.93	15.9	0.91
Stripping	–	<0	1	99.9	25.2	0.81
Total process				55.1	82.9	5.06

The process constructed by the ACO-based algorithm for the direct leaching method consists of three steps. The time for leaching step with H_2SO_4 is 150 min (corresponding pH of leachate is 3.0). The second step is solvent extraction with D2EHPA at pH 4.3. Finally, the loaded organic phase is stripped with the electrolyte without neutralization. The initially specified final purity of Zn (99.6%) in the electrolyte is not achieved (96.3%) that is also indicated from the total PPI value. The PPI value was 68.5%. The PPI should normally be equal to 100% when the specified target purity is reached. The composition of the final

purified solution is presented in Table 2. The concentrations of the contaminating elements in the final solution are higher than the required limits, though the calculated concentration of Zn in the purified solution is higher than initially specified (86.6 g/L). The impurities that are more electronegative than Zn, e.g. K, Na, Ca, Mg and Mn, do not directly interfere with the electrolytic process and can be tolerated up to 60 g/L. The impurities that are more electropositive than Zn, e.g. Fe, Ni, Cr and Pb lead to a reduction in the overvoltage, decrease in the current yield and deterioration of cathode purity (Habashi, 1997). For this reason, the maximum tolerable concentrations of these impurities are very low. Although the selected extractant for purification of the AOD leachate, D2EHPA, is characterized by its high capacity and selectivity for Zn over a wide range of common metals (Tsakiridis et al., 2010), the concentrations of Fe and Ni exceed the specified limits, and consequently the obtained electrolyte cannot be readily used in the electrolysis of Zn.

From the data for direct method (Fig. A1 in Appendix A) it can be seen that Fe would eventually precipitate away from the solution as the pH increases over 3, but there was still 1000 mg/L left after one day. Thus a similar process, but the first step is the previously introduced controlled leaching, was also optimized. Leaching time was optimized to be 270 min, and the solvent extraction and stripping steps are exactly the same as in the process with the direct leaching This process with controlled leaching is characterized by higher specific costs (controlled leaching 5.06 €/kg, direct leaching 3.61 €/kg) resulting from lower leaching yield, but it provides the electrolyte with permissible concentrations of impurities although the overall purity target was not reached. Though this case study clearly reveals the power of the constructed ACO-based algorithm in the hydrometallurgical process design, the previous discussion shows that the algorithm needs to be modified to use values of individual impurity components as boundary conditions if needed.

The most important characteristics for process performance of the constructed purification sequence for direct leaching process are presented in Table 3. It is worth noting that the values of the enrichment factors for solvent extraction with D2EHPA indicate considerable purification of Zn during the one step solvent extraction stage of the process. In practice, solvent extraction is carried out in cascades of two or more stages. The algorithm could be readily extended to handle also such multiple process steps in one unit process layer, and calculation of the PPI values could even involve dynamic simulations.

Table 3. Characteristics of extraction-back extraction part (25% v/v D2EHPA in kerosene) of the synthesized direct leaching process for Zn recovery from AOD dust.

	Zn	Ni	Fe	Ca	Cr	K	Mn	Mg
				Extraction				
Distribution coefficient	1385	0.01	1000	3.61	0.05	0.05	5.25	0.25
Enrichment factor for Zn over metal M	1	85	1	1.3	19	20	1.2	5
				Back extraction				
Stripping coefficient	6330	1662	1000	1000	1000	1000	1003	1050
Enrichment factor for Zn over metal M	1	1	1	1	1	1	1	1

The calculated specific production cost (5.06 €/kg), is higher than the market price of Zn (1.94 €/kg according to LME). It should be borne in mind, however, that the separation cost indicator is as such not intended for calculation of production costs but rather as a fast tool for comparison of process alternatives during the process concept synthesis stage of process development (Winkelnkemper and Schembecker, 2010).

3.2. Recovery of lanthanides from nickel metal hydride (NiMH) batteries

Present-day NiMH batteries contain multicomponent alloys such as $La_{0.8}Nd_{0.2}Co_{2.4}Si_{0.1}$, $La_{0.8}Nd_{0.2}Ni_{2.5}Co_{2.4}Al_{0.1}$, $MmNi_{3.55}Co_{0.75}Mn_{0.4}Al_{0.3}$ or $MmNi_{3.5}Co_{0.7}Al_{0.8}$ (where Mm refers to rare earth mischmetal) as the cathode and $Ni(OH)_2$ as the anode. In a recent comprehensive review of research on recycling of spent NiMH batteries (Binnemans et al., 2013), composition of the spent batteries is given as 36–42% Ni, 3–4% Co and 8–10% mischmetal containing La, Ce, Pr and Nd. The composition of raw material considered here is presented in Table 4. Lanthanides were chosen as target metals for their high value and relatively high content in the raw material. The target purity was set at 99% and the target phase as a solid precipitate.

The aim of this case study was to investigate the feasibility of the presented method to identify what should be the targets of each process step by utilizing data collected from literature sources. More specifically, the ACO based method was used to analyze whether it is better to design the first process steps such that high yield or high purity is achieved. High purity in leaching is usually achieved only by sacrificing the yield but this may be desired if the subsequent purification costs dictate the total costs.

Table 4. Composition of the raw material for the lanthanides recovery process from spent nickel metal hydride batteries (Zhang et al., 1998) and metal content of the precipitated oxalates.

	Ni	Co	Fe	Zn	Al	Mn	La	Ce	Pr	Nd	Sm
Raw material, %	64.3	4.5	7.7	2.4	1.1	2.7	9.2	0.6	1.8	5.8	0.2
Product (oxalates), %	<0.01	<0.01	<0.01	<0.01	<0.01	0.04	52	3.4	10.2	33	1.0

Potential mass separating agents were selected based on the literature (Zhang et al., 1998; Fernandes et al., 2013). HCl for leaching and stripping of the loaded organic phase, 25% v/v D2EHPA in kerosene for solvent extraction, and oxalic acid for precipitation of metals from the stripped aqueous solution. The data required for the calculations are presented in Appendix B. The calculations for specific leaching and purification costs were based on the chemistry of the processes and were performed in the same manner as in the case study for Zn recovery from AOD dust. The problem to be solved consisted of four layers with four unit operations and eight discrete values of operating parameters. The number of alternative processes and operating parameter combinations was approximately $1.1 \cdot 10^6$.

Table 5. Synthesized process for recovery of lanthanides from nickel metal hydride batteries using ACO-based algorithm. A stands for aqueous, O for organic and S for solid.

Unit operation	pH	Target phase	[HCl]	O/A	Yield, %	PPI, %	SCI, €/kg
Leaching	–	A	1.3	–	90.0	3.3	57.70
SX	2.2	O	–	1	99.8	33.5	2.63
Stripping	–	A	2.0	1	99.99	18.7	2.61
Precipitation	0.6	S	–	–	100	98.2	3.33
Total process					88.7	153.7	66.27

The constructed hydrometallurgical process sequence for recovery of lanthanides from Ni-MH batteries is presented in Table 5. The first step is leaching with 1.3 M HCl. The collected leachate is then contacted with 25% D2EHPA in kerosene at equilibrium pH 2.2 (O:A = 1:1). The loaded organic phase is then stripped with 2.0 M HCl (O:A = 1:1). The final step of the process is precipitation with oxalic acid at pH 0.6. The resulting metal oxalates (99% of REE, Mn as a contaminant) can be used for production of corresponding oxides. High specific leaching costs result from low purity improvement (PPI = 3.3%) in the leaching step, while the total process PPI indicates exceeding of initially specified target purity. The changes in metal purities over the process sequence are shown in Fig. 4. The organic phase is mostly

loaded with lanthanides, Fe and Zn. The raffinate after solvent extraction contains mostly Ni, Co, Fe and Mn.

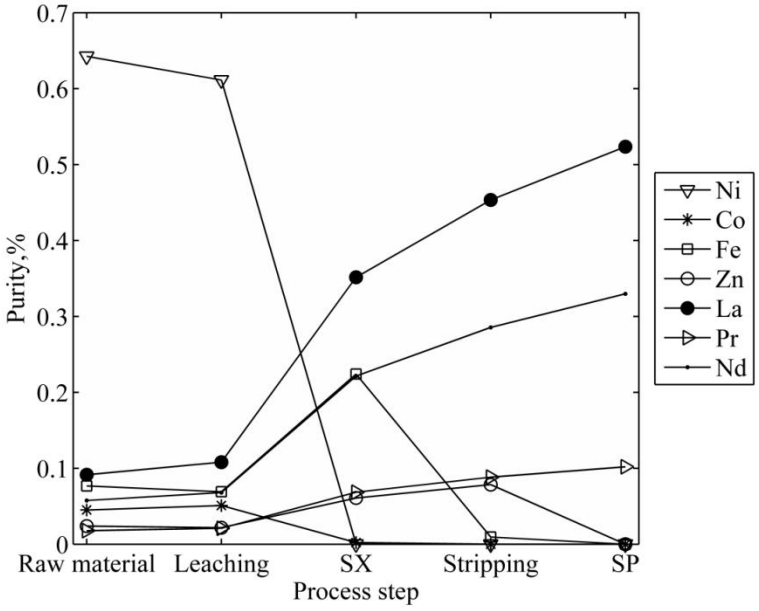

Figure 4. Changes in metal purities in the constructed process for lanthanides recovery from spent nickel metal hydride batteries. Characteristics of the process steps are presented in Table 5.

The constructed process resembles the conceptual flowsheet presented by Zhang et al. (1998). The difference in the values of the leaching acidity can be explained by the fact that the strategy of Zhang et al. (1998) was to maximize the leaching yield for all the metals. Here the ACO-based algorithm suggests optimizing leaching conditions towards selective leaching of lanthanides. Here single stage batch unit operations are exclusively used in the constructed processes, whereas multi-stage counter-current solvent extraction was explored experimentally by Zhang et al. (1998). The different operational modes thus explain the difference in operating parameters for solvent extraction and stripping. In addition, in this study, the economic factor was taken into account when comparing different schemes for interconnecting unit operations, because it is important to consider the economics of a designed process from the early stages of the process development.

4. Conclusions

A simple and efficient process synthesis method applicable to the initial stages of hydrometallurgical process development was presented. The method consists of three parts: experimentally obtained data, an ant colony optimization based algorithm and key performance indicators (KPIs). The core of the method is use of the ACO-based algorithm that efficiently identifies the most promising process alternative in iterative manner. Experimental data are used for construction of the superstructure of process alternatives. The total process costs, estimated as sum of step specific costs (SCI), serve as the objective function.

The practical applicability of the method was successfully demonstrated by its application for synthesis of recovery processes for Zn from argon oxygen decarburization (AOD) dusts and

for recovery of lanthanides from spent nickel metal hydride (Ni-MH) batteries. The efficiency of the algorithm (measured as CPU time) for large problems originates from the fact that inefficient process alternatives are excluded from the iterative solution in the early stages. Besides hydrometallurgy, the method is considered applicable for the design of any chemical purification process that involves simultaneous selection of mass separation agents, definition of the operating parameters of the unit processes involved and selection of their sequence.

Acknowledgements

The work was part of METDUST project in Finnish Metals and Engineering Competence Cluster's (FIMECC) research program Energy and Life-cycle Efficient Metal Processes (ELEMET). The participating organizations were Lappeenranta University of Technology, Aalto University, University of Oulu, Outokumpu Oyj, Outotec Oyj and Boliden Oy.

References

Acevedo, J., & Pistikopoulos, E. N. (1998). Stochastic optimization based algorithms for process synthesis under uncertainty. *Computers & Chemical Engineering*, *22*(4–5), 647-671. doi:http://dx.doi.org/10.1016/S0098-1354(97)00234-2

Ahamed, T., Ottens, M., Nfor, B. K., van Dedem, G. W. K., & van der Wielen, L. A. M. (2006). A generalized approach to thermodynamic properties of biomolecules for use in bioseparation process design. *Fluid Phase Equilibria*, *241*(1–2), 268-282. doi:http://dx.doi.org/10.1016/j.fluid.2005.12.011

Alonso, A. I., Lassahn, A., & Gruhn, G. (2001). Optimal design of non-dispersive solvent extraction processes. *Computers & Chemical Engineering*, *25*(2–3), 267-285. doi:http://dx.doi.org/10.1016/S0098-1354(00)00652-9

Angira, R., & Babu, B. V. (2006). Optimization of process synthesis and design problems: A modified differential evolution approach. *Chemical Engineering Science*, *61*(14), 4707-4721. doi:http://dx.doi.org/10.1016/j.ces.2006.03.004

Bhambure, R., Kumar, K., & Rathore, A. S. (2011). High-throughput process development for biopharmaceutical drug substances. *Trends in Biotechnology*, *29*(3), 127-135. doi:http://dx.doi.org/10.1016/j.tibtech.2010.12.001

Binnemans, K., Jones, P. T., Blanpain, B., Van Gerven, T., Yang, Y., Walton, A., & Buchert, M. (2013). Recycling of rare earths: A critical review. *Journal of Cleaner Production*, *51*(0), 1-22. doi:http://dx.doi.org/10.1016/j.jclepro.2012.12.037

745 Biswas, A., Chakraborti, N., & Sen, P. K. (2009). A genetic algorithms based multi-objective
746 optimization approach applied to a hydrometallurgical circuit for ocean nodules. *Mineral*
747 *Processing and Extractive Metallurgy Review, 30*(2), 163-189.
748 doi:http://dx.doi.org/10.1080/08827500802397284

749 Blum, C. (2005). Ant colony optimization: Introduction and recent trends. *Physics of Life*
750 *Reviews, 2*(4), 353-373. doi:http://dx.doi.org/10.1016/j.plrev.2005.10.001

751 Chakraborty, A., Purkarthofer, K. A., & Linninger, A. A. (2004). Conceptual design of
752 metallurgical processes based on thermodynamic and economic insights. *Chemical*
753 *Engineering and Processing: Process Intensification, 43*(5), 625-640.
754 doi:http://dx.doi.org/10.1016/j.cep.2003.02.004

755 Chunfeng, W., & Xin, Z. (2002). Ants foraging mechanism in the design of multiproduct
756 batch chemical process. *Industrial and Engineering Chemistry Research, 41*(26), 6678-6686.
757 doi:http://dx.doi.org/10.1021/ie010932r

758 Cisternas, L. A. (1999). On the synthesis of inorganic chemical and metallurgical processes,
759 review and extension. *Minerals Engineering, 12*(1), 15-41.
760 doi:http://dx.doi.org/10.1016/S0892-6875(98)00117-4

761 Cytec, A closer look at reagent consumption, 2006, https://www.cytec.com/specialty-
762 chemicals/PDFs/SolventExtraction/ReagentConsumptionInCuSX.pdf (Accessed 31.10.2013).

763 Cziner, K., Virkki-Hatakka, T., Hurme, M., & Turunen, I. (2005). Evaluative approach for
764 process development. *Chemical Engineering & Technology, 28*(12), 1490-1499.
765 doi:http://dx.doi.org/10.1002/ceat.200500212

766 Fernandes, A., Afonso, J. C., & Dutra, A. J. B. (2013). Separation of nickel(II), cobalt(II) and
767 lanthanides from spent Ni-MH batteries by hydrochloric acid leaching, solvent extraction and
768 precipitation. *Hydrometallurgy, 133*(0), 37-43.
769 doi:http://dx.doi.org/10.1016/j.hydromet.2012.11.017

770 Forsén, O., & Aromaa, J. (2013). The use of hydrometallurgy in treatment of secondary raw
771 materials and low-grade ores. *Acta Metallurgica Slovaca, 19*(3), 184-195.
772 doi:http://dx.doi.org/10.12776/ams.v19i3.160

773 Gálvez, E. D., Vega, C. A., Swaney, R. E., & Cisternas, L. A. (2004). Design of solvent
774 extraction circuit schemes. *Hydrometallurgy, 74*(1–2), 19-38.
775 doi:http://dx.doi.org/10.1016/j.hydromet.2003.10.005

776 Grossmann, I. E., Caballero, J. A., & Yeomans, H. (1999). Mathematical programming
777 approaches to the synthesis of chemical process systems. *Korean Journal of Chemical*
778 *Engineering, 16*(4), 407-426. doi:http://dx.doi.org/10.1007/BF02698263

779 Grossmann, I. E., & Daichendt, M. M. (1996). New trends in optimization-based approaches
780 to process synthesis. *Computers & Chemical Engineering, 20*(6–7), 665-683.
781 doi:http://dx.doi.org/10.1016/0098-1354(95)00201-4

782 Habashi, F. (1997). Primary metals. In F. Habashi (Ed.), *Handbook of extractive metallurgy,*
783 *volum 2* (pp. 491-794). Weinheim, Germany: WILEY-VCH, 1997.

784 Havlik, T., Turzakova, M., Stopic, S., & Friedrich, B. (2005). Atmospheric leaching of EAF
785 dust with diluted sulphuric acid. *Hydrometallurgy, 77*(1–2), 41-50.
786 doi:http://dx.doi.org/10.1016/j.hydromet.2004.10.008

787 Linninger, A. A. (2002). Metallurgical process design - A tribute to douglas' conceptual
788 design approach. *Industrial and Engineering Chemistry Research, 41*(16), 3797-3805.
789 doi:http://dx.doi.org/10.1021/ie0107901

790 LME (2014), London metal exchange: Zinc Retrieved from http://www.lme.com/en-
791 gb/metals/non-ferrous/zinc/ (Accessed 19.3.2014).

792 Marchenko, N. V. (2009). Electrolysis of zinc. In N. V. Marchenko, E. P. Vershinina & E. M.
793 Gildebrandt (Eds.), *Metallurgy of heavy non-ferrous metals* (pp. 149-158). Krasnoyarsk:
794 Siberian Federal University.

795 Nfor, B. K., Verhaert, P. D. E. M., van der Wielen, L. A. M., Hubbuch, J., & Ottens, M.
796 (2009). Rational and systematic protein purification process development: The next
797 generation. *Trends in Biotechnology, 27*(12), 673-679.
798 doi:http://dx.doi.org/10.1016/j.tibtech.2009.09.002

799 Nienow, A. W. (1997). Chapter 16 - the suspension of solid particles. In N. Harnby, M. F.
800 Edwards & A. W. Nienow (Eds.), *Mixing in the process industries* (pp. 364-393). Oxford:
801 Butterworth-Heinemann. doi:http://dx.doi.org/10.1016/B978-075063760-2/50037-8

802 Oustadakis, P., Tsakiridis, P. E., Katsiapi, A., & Agatzini-Leonardou, S. (2010).
803 Hydrometallurgical process for zinc recovery from electric arc furnace dust (EAFD): Part I:
804 Characterization and leaching by diluted sulphuric acid. *Journal of Hazardous Materials,*
805 *179*(1–3), 1-7. doi:http://dx.doi.org/10.1016/j.jhazmat.2010.01.059

806 Pereira, D. D., Rocha, S. D. F., & Mansur, M. B. (2007). Recovery of zinc sulphate from
807 industrial effluents by liquid–liquid extraction using D2EHPA (di-2-ethylhexyl phosphoric
808 acid). *Separation and Purification Technology, 53*(1), 89-96.
809 doi:http://dx.doi.org/10.1016/j.seppur.2006.06.013

810 Preston, J. S. (1985). Solvent extraction of metals by carboxylic acids. *Hydrometallurgy,*
811 *14*(2), 171-188. doi:http://dx.doi.org/10.1016/0304-386X(85)90032-5

812 Raeesi, B., Pishvaie, M. ?., & Rashtchian, D. (2008). Optimization of a process synthesis
813 superstructure using an ant colony algorithm. *Chemical Engineering & Technology, 31*(3),
814 452-462. doi:http://dx.doi.org/10.1002/ceat.200700324

815 Rao, S. S. (1996). *Engineering optimization : Theory and practice* (3rd ed.). New York: John
816 Wiley & Sons, Inc.

817 Rintala, L., Lillkung, K., & Aromaa, J. (2011). The use of decision and optimization methods
818 in selection of hydrometallurgical unit process alternatives. *Physicochemical Problems of*
819 *Mineral Processing*, *46*, 229-242.

820 Robinson, C. G., & Paynter, J. C. (1971). Optimization of the design of a countercurrent
821 liquid-liquid extraction plant using LIX-64N. *Proceedings International Solvent Extraction*
822 *Conference 1971*, Hague. , *2* 1417-1428.

823 Rodríguez de San Miguel, E. R., Aguilar, J. C., Bernal, J. P., Ballinas, M. L., Rodríguez, M.
824 T. J., de Gyves, J., & Chimmel, K. (1997). Extraction of cu(II), fe(III), ga(III), ni(II), in(III),
825 co(II), zn(II) and pb(II) with LIX® 984 dissolved in n-heptane. *Hydrometallurgy*, *47*(1), 19-
826 30. doi:http://dx.doi.org/10.1016/S0304-386X(97)00042-X

827 Schuldt, S., & Schembecker, G. (2013). A fully automated ad- and desorption method for
828 resin and solvent screening. *Chemical Engineering & Technology*, *36*(7), 1157-1164.
829 doi:http://dx.doi.org/10.1002/ceat.201200725

830 Shawabkeh, R. A. (2010). Hydrometallurgical extraction of zinc from jordanian electric arc
831 furnace dust. *Hydrometallurgy*, *104*(1), 61-65.
832 doi:http://dx.doi.org/10.1016/j.hydromet.2010.04.014

833 Sreekrishnan, T. R., & Tyagi, R. D. (1996). A comparative study of the cost of leaching out
834 heavy metals from sewage sludges. *Process Biochemistry*, *31*(1), 31-41.
835 doi:http://dx.doi.org/10.1016/0032-9592(95)00019-4

836 Statistics Finland, Price of electricity by type of consumer, 2014,
837 http://www.stat.fi/til/ehi/2013/04/ehi_2013_04_2014-03-20_kuv_005_en.html (Accessed
838 1.6.2014).

839 Steimel, J., Harrmann, M., Schembecker, G., & Engell, S. (2013). Model-based conceptual
840 design and optimization tool support for the early stage development of chemical processes
841 under uncertainty. *Computers & Chemical Engineering*, *59*(0), 63-73.
842 doi:http://dx.doi.org/10.1016/j.compchemeng.2013.06.017

843 Trujillo, J. Y., Cisternas, L. A., Gálvez, E. D., & Mellado, M. E. (2014). Optimal design and
844 planning of heap leaching process. application to copper oxide leaching. *Chemical*
845 *Engineering Research and Design*, *92*(2), 308-317.
846 doi:http://dx.doi.org/10.1016/j.cherd.2013.07.027

847 Tsakiridis, P. E., Oustadakis, P., Katsiapi, A., & Agatzini-Leonardou, S. (2010).
848 Hydrometallurgical process for zinc recovery from electric arc furnace dust (EAFD). part II:
849 Downstream processing and zinc recovery by electrowinning. *Journal of Hazardous*
850 *Materials*, *179*(1–3), 8-14. doi:http://dx.doi.org/10.1016/j.jhazmat.2010.04.004

851 U.S. Energy Information Administration, U.S. Kerosene Wholesale/Resale Price by Refiners,
852 2014,
853 http://www.eia.gov/dnav/pet/hist/LeafHandler.ashx?n=PET&s=EMA_EPPK_PWG_NUS_D
854 PG&f=M (Accessed 2.6.2014).

US Bureau of Mines, Mineral processing – Operating costs, 2009, http://paulywogbog.net/Rebuilt%20460/Special%20Resources/US%20Bureau%20of%20Mines%20CES%20Mineral%20Processing/Mineral%20Processing%20Operating%20Costs%20Hydrometallurgy.PDF (Accessed 2.6.2014).

Virolainen, S., Salmimies, R., Hasan, M., Häkkinen, A., & Sainio, T. (2013). Recovery of valuable metals from argon oxygen decarburization (AOD) dusts by leaching, filtration and solvent extraction. *Hydrometallurgy, 140*(0), 181-189. doi:http://dx.doi.org/10.1016/j.hydromet.2013.10.002

Winkelnkemper, T., & Schembecker, G. (2010). Purification performance index and separation cost indicator for experimentally based systematic downstream process development. *Separation and Purification Technology, 72*(1), 34-39. doi:http://dx.doi.org/10.1016/j.seppur.2009.12.025

Zhang, P., Yokoyama, T., Itabashi, O., Wakui, Y., Suzuki, T. M., & Inoue, K. (1998). Hydrometallurgical process for recovery of metal values from spent nickel-metal hydride secondary batteries. *Hydrometallurgy, 50*(1), 61-75. doi:http://dx.doi.org/10.1016/S0304-386X(98)00046-2

Appendix A. Experimental data for case of Zn recovery from AOD dust

The experimental data used as an input in the ant colony optimization algorithm for the case of Zn recovery from AOD dust is presented in Figs. A1 to A5. The data were interpolated such that for each unit operation there were 30 levels of operating parameters. The pH isotherms for solvent extraction (Figs. A3-A5) are used for both extraction and stripping unit processes. The data produced by the research group of the current authors (the AOD case), have been presented in appendices both as figures and in tabular form (Figures A1 to A3, Tables A1 to A3). The data obtained from literature have been presented as they appear in the references.

882 Table A1. Direct leaching of AOD dust with 0.5 M H_2SO_4. L/S -ratio = 5:1 (L/kg), T = 30 °C. (For more details an interested reader is referred
883 to Virolainen et al., 2013.)

Time, min	pH	Leaching concentration, $mg \cdot L^{-1}$								
		Zn	Ni	Fe	Ca	Cr	K	Mn	Mg	Pb
0	0.6	0.00	0.00	0.00	0.00	0.00	0.00	0.00	0.00	0.00
15	2.48	12584.23	46.18	2427.56	610.89	463.05	1356.16	796.03	1720.35	19.16
30	2.57	12812.89	48.38	2053.90	590.61	452.78	1348.70	846.24	1755.74	18.12
45	2.62	13032.74	56.06	1936.92	593.60	455.16	1416.32	910.42	1846.68	19.29
60	2.7	13428.9	57.89	1830.70	610.40	450.56	1426.17	936.30	1892.25	17.69
90	2.76	12846.78	56.96	1631.62	596.65	402.62	1353.75	887.80	1786.75	16.90
120	2.90	12996.41	61.22	1560.54	596.03	386.40	1378.18	907.49	1819.28	16.44
150	3.03	13672.12	66.38	1565.40	600.14	388.84	1436.44	955.21	1929.95	15.64
180	3.14	13118.07	64.90	1487.11	588.23	298.65	1408.78	936.17	1915.49	15.36
240	3.33	13554.36	67.40	1528.67	601.72	283.48	1464.42	1003.81	1993.86	14.35
300	3.53	13744.57	69.00	1377.77	607.13	260.75	1389.37	984.99	1892.09	14.04
360	3.66	13519.86	69.80	1392.42	583.84	235.97	1385.87	982.18	1925.12	14.38
420	3.78	13160.73	68.32	1331.95	573.10	213.10	1307.08	949.88	1861.66	14.23
1440	4.17	13222.51	75.21	1020.13	540.28	73.76	1369.02	1013.18	2004.87	14.59

884

885 Table A2. Leaching of AOD dust with H_2SO_4 and controlled pH of the solution by keeping the pH close to, but above, 3.0 with 96% H_2SO_4.
886 L/S -ratio = 5:1 (L/kg), T = 30 °C. (For more details an interested reader is referred to Virolainen et al., 2013.)

Time, min	pH	Leaching concentration, $mg \cdot L^{-1}$								
		Zn	Ni	Fe	Ca	Cr	K	Mn	Mg	Pb
0	3.00	0.00	0.00	0.00	0.00	0.00	0.00	0.00	0.00	0.00
1	6.28	449.15	1.00	0.00	1644.18	221.21	971.71	13.22	50.83	15.30
4	5.60	1691.79	1.00	0.00	845.90	214.03	949.45	25.57	122.51	15.09
8	4.99	4683.18	1.00	0.00	687.23	246.43	1120.83	65.92	363.72	12.93
13	4.90	6540.16	1.64	0.00	636.92	245.17	1163.25	100.44	658.54	11.24
18	4.81	6159.71	2.26	0.00	585.92	208.19	1007.04	101.43	732.97	10.08
25	4.24	7522.20	2.89	0.00	563.22	215.41	1018.44	128.09	920.16	12.07
40	4.09	8860.97	6.01	0.00	518.38	198.51	966.70	169.10	1145.51	12.82
50	3.84	9617.95	6.79	0.00	498.27	196.19	984.36	180.17	1252.31	12.53
60	3.60	10609.29	7.72	0.00	521.17	206.05	984.43	188.60	1322.68	13.80
90	3.30	10236.05	9.72	0.00	510.53	212.38	967.45	200.43	1383.02	11.92
120	3.30	9853.42	10.51	0.00	501.29	209.01	912.39	204.47	1360.03	12.88
190	3.02	10220.00	12.97	0.00	511.62	219.95	930.47	236.41	1448.77	13.49
225	3.07	10725.31	15.36	0.00	534.11	242.46	1079.87	278.44	1671.35	10.12
240	3.14	10278.58	14.09	0.00	495.31	207.42	947.33	249.22	1458.18	11.95
270	3.17	10959.71	14.94	0.00	512.70	215.89	978.36	271.39	1556.23	15.12

887 Table A3. Solvent extraction of metals with D2EHPA from solution obtained from 0.5 M H_2SO_4 leaching of AOD dust. T = 30 °C, O/A = 1:1.
888 (For more details an interested reader is referred to Virolainen et al., 2013.)

pH	Extraction, %								
	Zn	Ni	Fe	Ca	Cr	K	Mn	Mg	Pb
-0.57	99.90	99.90	99.90	99.90	99.90	99.90	99.90	99.90	0.00
-0.20	99.90	99.90	99.90	99.90	99.90	99.90	99.90	99.90	0.00
0.01	99.90	99.90	99.90	99.90	99.90	99.90	99.90	99.90	0.00
0.20	96.22	99.90	92.52	99.46	99.05	99.90	99.90	99.90	0.00
0.50	78.94	99.90	60.00	99.90	99.90	96.88	98.58	97.78	0.00
1.00	48.92	98.10	20.96	90.49	98.07	99.90	98.84	99.77	0.00
1.52	23.21	96.69	17.09	92.17	98.68	96.97	98.31	99.30	0.00
2.00	11.20	97.16	0.00	89.98	98.05	96.19	94.02	96.96	0.00
2.55	2.88	99.27	0.00	82.10	99.35	98.18	90.89	99.90	0.00
2.98	1.21	98.38	0.00	65.30	99.90	96.28	74.46	99.01	0.00
3.52	0.80	98.60	0.00	40.98	98.94	95.76	44.19	96.44	0.00
4.08	0.04	99.90	0.00	25.57	97.63	93.51	21.00	85.11	0.00
4.50	0.11	97.47	0.00	17.22	91.57	96.71	10.24	74.12	0.00
5.08	2.34	97.58	0.00	12.56	71.80	95.50	6.55	53.24	0.00
5.51	0.15	95.41	0.00	5.07	47.95	96.36	0.00	42.08	0.00
6.56	7.18	74.25	0.00	9.20	11.74	96.88	9.00	35.01	0.00

7.56	0.54	46.96	0.00	2.88	0.00	98.61	0.00	30.49	0.00
8.51	4.71	46.99	0.00	1.02	1.50	96.71	0.00	27.99	0.00
8.85	25.84	52.77	0.00	0.00	0.00	97.92	0.00	25.20	0.00

889

890

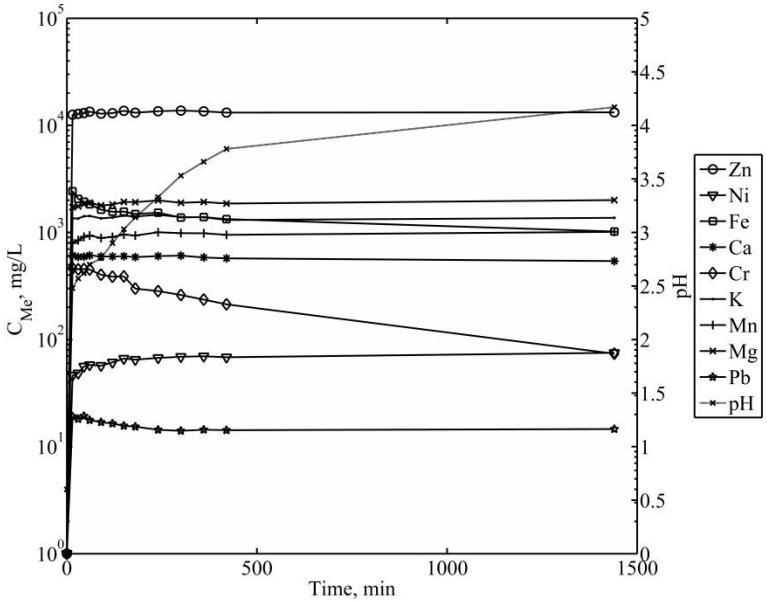

891

892 Fig. A1. Direct leaching of AOD dust with 0.5 M H_2SO_4. L/S -ratio = 5:1 (L/kg),
893 T = 30 °C. (For more details an interested reader is referred to Virolainen et al., 2013.)

894

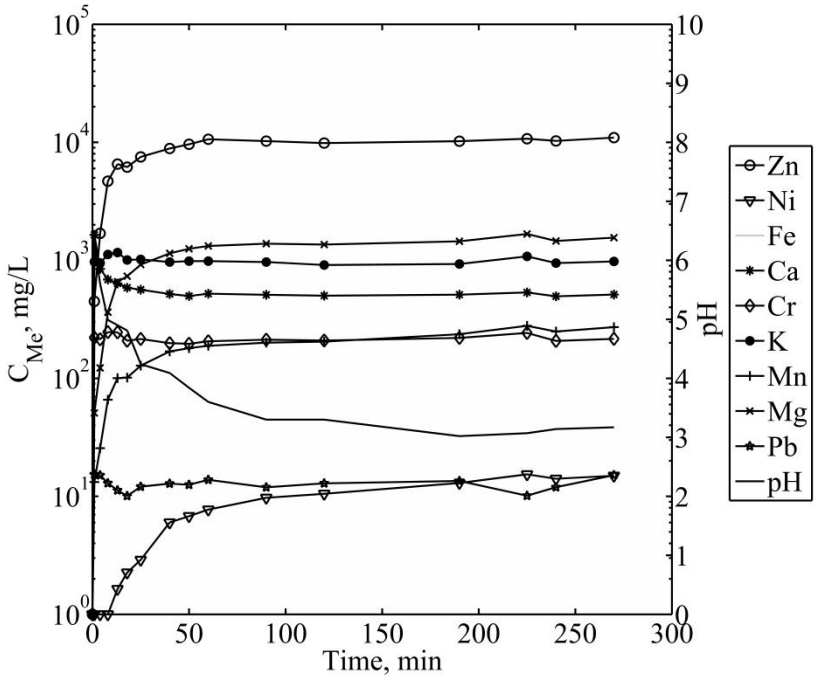

Fig. A2. Leaching of AOD dust with H_2SO_4 and controlled pH of the solution by keeping the pH close to, but above, 3.0 with 96% H_2SO_4. L/S -ratio = 5:1 (L/kg), T = 30 °C. (For more details an interested reader is referred to Virolainen et al., 2013.)

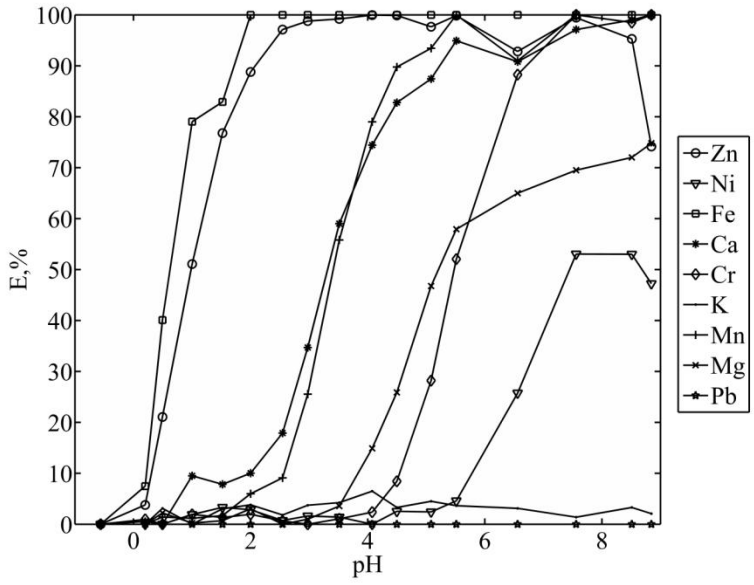

Fig. A3. Solvent extraction of metals with D2EHPA from solution obtained from 0.5 M H_2SO_4 leaching of AOD dust. T = 30 °C, O/A = 1:1. (For more details an interested reader is referred to Virolainen et al., 2013.)

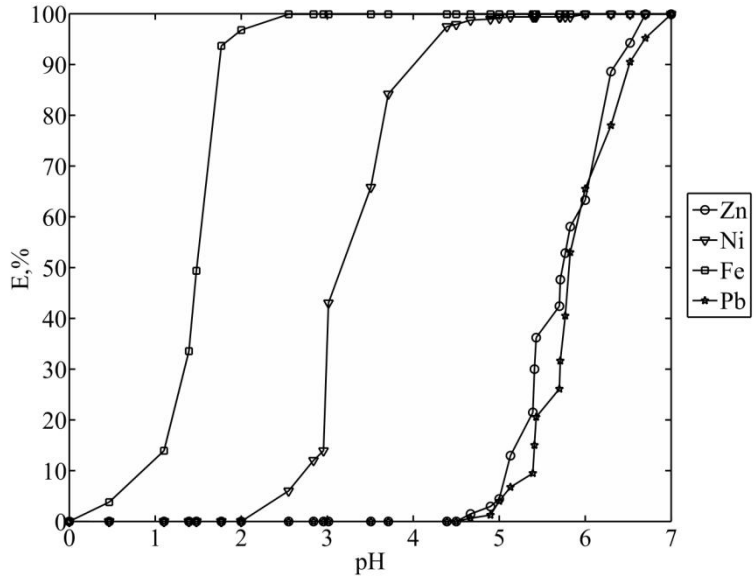

905

906 Fig. A4. Percent of extraction of 20 ppm of metal ions as a function of the equilibrium pH
907 of the aqueous phase with 0.3 M hydroxyoxime LIX 984 at T=25°C. (For more
908 details an interested reader is referred to Rodríguez de San Miguel et al., 1997.)

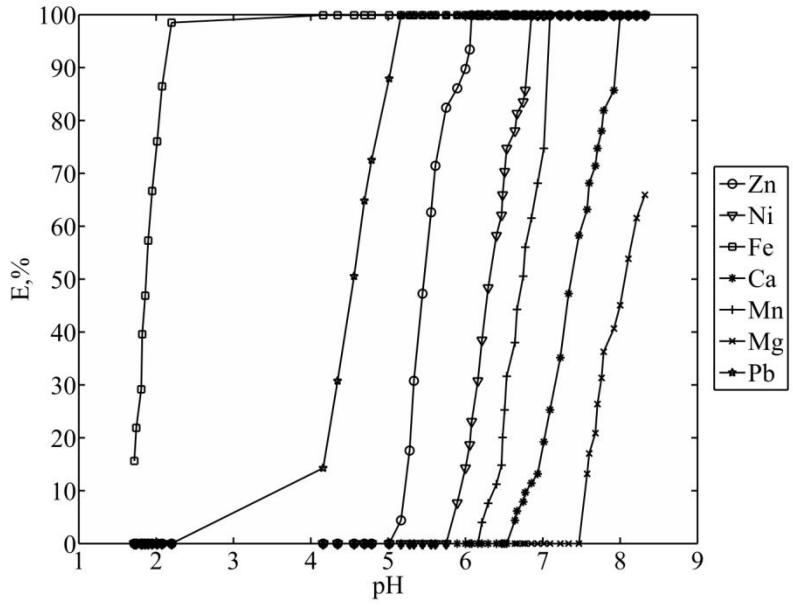

909

910 Fig. A5. Solvent extraction of some metals with 0.50 M solution of Versatic 10 acid in
911 xylene at 20°C. (For more details an interested reader is referred to Preston,
912 1985.)
913

914 # Appendix B. Experimental data for case of lanthanides recovery from
915 # spent NiMH batteries

916 The experimental data used as an input in the ant colony optimization algorithm for the case
917 of lanthanides recovery from spent NiMH batteries is presented in Tables B1 to B2 and Figs.
918 B1 to B2. The data were interpolated such that for each unit operation there were 8 levels of
919 operating parameters.

920 Table B1. Effect of HCl concentration and O:A phase ratio on stripping of some metals
921 from D2EHPA at 25°C. Solvent loading (g L^{-1}): [RE]=2.65, [Mn]=0.34,
922 [Zn]=0.22, [Al]=0.15, [Fe]=1.15. (For more details an interested reader is referred
923 to Zhang et al., 1998.)

	Stripping yields of metals, %							
[HCl], mol/L	1.0	1.5	2.0	3.0	2.0	2.0	2.0	2.0
O:A ratio	1:1	1:1	1:1	1:1	2:1	3:1	5:1	10:1
Ni	0.01	0.01	0.01	0.01	0.01	0.01	0.01	0.01
Co	0.01	0.01	0.01	0.01	0.01	0.01	0.01	0.01
Fe	0.27	1	3.3	17.9	1.3	0.5	0.4	0.1
Zn	96.4	98.7	99.99	99.99	99.99	99.99	99.99	99.99
Al	48	69.3	78	99.99	59.7	41.2	37.5	35.9
Mn	99.99	99.99	99.99	99.99	99.99	99.99	99.99	99.99
REE	97.3	99.4	99.99	99	99.99	99.99	99.5	97.6

924

925

926 Table B2. The effect of pH on precipitation of some metals as oxalates by addition of
927 0.3 mol L^{-1} $(NH_4)_2C_2O_4$ at 60°C, under stirring (200 rpm). (For more details an
928 interested reader is referred to Fernandes et al., 2013.)

	Extraction yields of metals, %					
pH	0	0,5	1	2	3	4
Ni	0	0	0	23	99.6	99.7
Co	0	0	0	99.99	99.99	99.99
Fe	0	0	0	0	0	0
Zn	0	0	0	0	0	0
Al	0	0	0	0	0	0
Mn	0	0	10	25	99.99	99.99
REE	50	98.5	99.9999	99.99	99.99	99.99

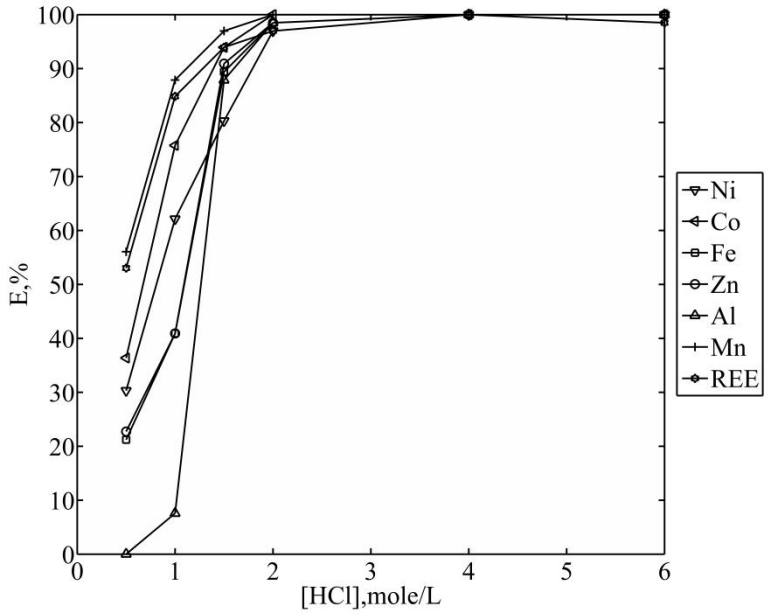

929

930 Fig. B1. Effect of HCl concentration on leaching of metals from spent NiMH batteries
931 (temperature=95°C, *t*=2 h). (For more details an interested reader is referred to
932 Zhang et al., 1998.)

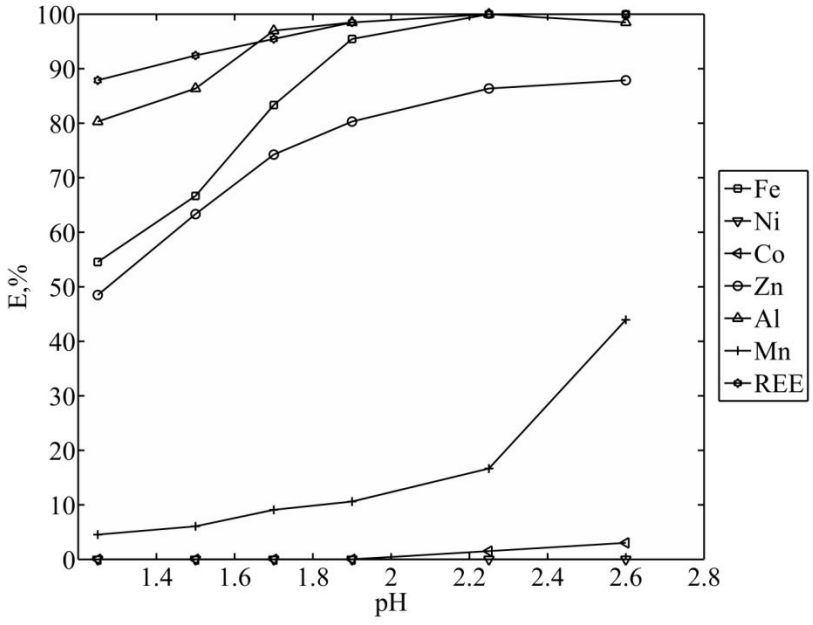

933

934 Fig. B2. Solvent extraction of metals from the leachate of spent NiMH batteries with 25%
935 D2EHPA in kerosene at O:A=1 and at 25°C. (For more details an interested
936 reader is referred to Zhang et al., 1998.)